


The efficacy of lapatinib and nilotinib in combination with radiation therapy in a model of NF2 associated peripheral schwannoma

Iddo Paldor¹ · Sara Abbadi¹ · Nicolas Bonne⁷ · Xiaobu Ye¹ · Fausto J. Rodriguez^{3,6} · David Rowshanshad¹ · MariaLisa Itzoe¹ · Veronica Vigilar¹ · Marco Giovannini⁸ · Henry Brem^{1,3,4,5} · Jaishri O. Blakeley^{1,2,3} · Betty M. Tyler¹ 

Received: 15 February 2017 / Accepted: 13 July 2017 / Published online: 22 July 2017
© Springer Science+Business Media, LLC 2017

Abstract Neurofibromatosis type 2 (NF2), a neuro-genetic condition manifest by peripheral nerve sheath tumors (PNST) throughout the neuroaxis for which there are no approved therapies. In vitro and in vivo studies presented here examine agents targeting signaling pathways, angiogenesis, and DNA repair mechanisms. In vitro dose response assays demonstrated potent activity of lapatinib and nilotinib against the mouse schwannoma SC4 (*Nf2*^{-/-}) cell line. We then examined the efficacy of everolimus, nilotinib, lapatinib, bevacizumab and radiation (RT) as mono- and combination therapies in flank and sciatic nerve in vivo NF2-PNST models. Data were analyzed using generalized linear models, two sample T-tests and paired T-tests, and linear regression models. SC4(*Nf2*^{-/-})

cells implanted in the flank or sciatic nerve showed similar rates of growth ($p=0.9748$). Lapatinib, nilotinib and RT significantly reduced tumor growth rate versus controls in the in vivo flank model ($p=0.0025$, 0.0062 , and 0.009 , respectively) whereas bevacizumab and everolimus did not. The best performers were tested in the in vivo sciatic nerve model of NF2 associated PNST, where chemoradiation outperformed nilotinib or lapatinib as single agents (nilotinib vs. nilotinib + RT, $p=0.0001$; lapatinib versus lapatinib + RT, $p<0.0001$) with no observed toxicity. There was no re-growth of tumors even 14 days after treatment was stopped. The combination of either lapatinib or nilotinib with RT resulted in greater delays in tumor growth rate than any modality alone. This data suggest that concurrent low dose RT and targeted therapy may have a role in addressing progressive PNST in patients with NF2.

✉ Betty M. Tyler
btyler@jhmi.edu

¹ Departments of Neurosurgery, Johns Hopkins University School of Medicine, Baltimore, MD, USA

² Departments of Neurology, Johns Hopkins University School of Medicine, Baltimore, MD, USA

³ Departments of Oncology, Johns Hopkins University School of Medicine, Baltimore, MD, USA

⁴ Departments of Ophthalmology, Johns Hopkins University School of Medicine, Baltimore, MD, USA

⁵ Departments of Biomedical Engineering, Johns Hopkins University School of Medicine, Baltimore, MD, USA

⁶ Departments of Pathology, Johns Hopkins University School of Medicine, Baltimore, MD, USA

⁷ Department of Otolaryngology and Neurotology, University Hospital of Lille, and INSERM U1008, University of Lille, Lille, France

⁸ Department of Head and Neck Surgery, David Geffen School of Medicine at UCLA, Los Angeles, CA, USA

Keywords Lapatinib · Nilotinib · Radiation · Peripheral schwannoma

Introduction

Neurofibromatosis type 2 (NF2) is a rare neurogenetic syndrome inherited in an autosomal dominant fashion [1]. It manifests with multiple nervous system tumors, including schwannomas, meningiomas, and ependymomas [1]. The causative mutation is in the *NF2* gene on chromosome 22q11.2, which leads to inactivation of the tumor suppressor protein merlin [2–4]. The absence of normal merlin has been shown to decrease apoptosis, lead to abnormal angiogenesis, and increase proliferation indices in Schwann cells [5, 6].

The majority of therapeutic discovery efforts for NF2 associated tumors have focused on vestibular schwannomas

(VS) as these are pathognomonic for the syndrome and often result in early deafness [7, 8]. However, patients with NF2 develop progressive neurologic morbidity from other peripheral schwannomas as well. Current treatment of symptomatic sporadic peripheral nerve sheath tumors (PNST) such as schwannomas consists of surgical resection and in some cases, focal radiation therapy (RT) [9]. In the setting of NF2, there is concern that RT may have a risk of malignant conversion and often the number of PNST make surgery impractical. There are no known effective drug therapies for these tumors.

Recent clinical experiences with bevacizumab for VS indicate that just under 40% of NF2-associated VS respond to bevacizumab [10]. Everolimus (RAD001), an inhibitor of the mammalian target of rapamycin (mTOR), has been used clinically to treat cancer subtypes such as metastatic renal cell carcinoma [11], neuroendocrine tumors [12], and breast cancer [13]. It has also been shown to delay tumor growth in a xenograft model of malignant peripheral nerve sheath tumors and in NF2 associated schwannomas [14]. Based on this encouraging pre-clinical data, everolimus was advanced to clinical studies for NF2 associated progressive VS where it has been shown to delay tumor progression for a subset of patients. For example, in one study 5 out of 9 patients had a decrease in the median annual growth rate from 67%/year before treatment to 0.5%/year during treatment, suggesting that everolimus is having a biologic effect on VS despite lack of radiographic or hearing response [15–17]. Similarly, lapatinib, an inhibitor of the epidermal growth factor receptor (EGFR) and downstream effector proteins ErbB2 and ErbB3, has been used extensively to treat breast cancer in humans [18] and has demonstrated inhibition of human schwann cell proliferation in vitro [19, 20]. It was therefore tested in children and adults with progressive NF2 associated VS and resulted in partial tumor reduction in 4 out of 17 patients (24%) [21]. PNST response was not evaluated. Finally, nilotinib, which inhibits the Bcr/Abl pathway, is a platelet derived growth factor C-kit cascade inhibitor and has demonstrated efficacy in the treatment of chronic myeloid leukemia (CML) [22] and gastro-intestinal stromal tumors [23]. Nilotinib has also demonstrated efficacy in vitro against NF2 related schwannoma cell lines [24] and is a well-tolerated oral agent that is being considered for clinical trials for NF2 associated tumors.

The role of RT in treating peripheral schwannomas is unclear. Although it is advocated by some for the treatment of sporadic PNST, there is a lack of data about toxicity or efficacy for NF2 associated PNST. The available data regarding RT for NF2 associated VS indicates that there are lower rates of tumor control or maintenance of hearing and higher rates of complications in the setting of NF2 associated VS versus sporadic VS [25, 26]. A recent

pre-clinical study demonstrated improved tumor control with anti-VEGF treatment plus RT compared to either modality alone for intracranial schwannomas [27]. This raises the possibility that chemoradiation may have benefit for NF2 associated PNST as well.

The treatment agents discussed above have mechanisms of action and targets pertinent to NF2 associated tumors, have shown activity (pre-clinical or clinical) in NF2 associated VS, and have the potential to be rapidly translated to the clinical setting. However, none has been evaluated for their efficacy against NF2 associated PNST and there is very little data available regarding the toxicity or efficacy of these agents used in combination with RT. This study evaluated each of the most promising therapies for NF2 VS as single agent therapy for NF2 associated PNST. We then advanced the most promising compounds for combination testing with RT in an effort to identify therapies that may be effective against non-vestibular PNST in people with NF2.

Materials and methods

Animals and materials

All research protocols were approved by the Institutional Animal Care and Use Committee of Johns Hopkins University. Nu/nu mice were acquired from Harlan BioProducts (Indianapolis, Indiana). The animals were housed in the Johns Hopkins University research animal facility, with 12 h sleep/wake cycles and free access to food and water. Bevacizumab, purchased from Genentech, Inc. (San Francisco, CA), was tested as described previously in other rodent models [28–30]. Everolimus was acquired from Novartis Pharmaceuticals Corporation (East Hanover, NJ) and nilotinib and lapatinib were purchased from Euroasian Chemicals Pvt. Ltd (Mumbai, India).

NF2 related schwannoma cell line

The origin of the SC4 cell line is a mouse adult Schwann cell line from *Nf2*^{-loxP} mice, with the second allele deleted in vitro using adeno-cre resulting in *Nf2*^{-/-} genotype. These cells were obtained through a Material Transfer Agreement with House Research Institute (Los Angeles, California). Cells were transfected with a plasmid encoding a fusion EGFP luciferase gene under the control of the CMV promoter. Cells were maintained in Dulbecco's modified eagle medium, supplemented by 10% fetal bovine serum, 1% penicillin/streptomycin, and 1% L-Glutamine and cultured at 37 °C in a 5% CO₂ environment.

In vitro irradiation study

Cells were plated in a monolayer in 6-well plates at a cell density of 100,000 cells/well. 4 days after plating, following confirmation by microscope of partial confluence of the cells, each plate was treated with a single dose of RT at 1 of 6 doses: 0, 1, 2, 5, 10 and 20 Gy (Gammacell 40 irradiator, Best Theratronics, ON, Canada). This dosing regimen was intended to mimic clinically-utilized stereotactic RT. 5 days later cells were trypsinized and counted in an automated cell counter [Vi-Cell XR Cell Viability Analyzer (Beckman Coulter, Indianapolis, IN)]. Data acquired was calculated and analyzed as a percent of the untreated control plate and a radiation dose response curve was obtained. The dose of RT that killed half of the cells in these studies was defined as the IC50.

In vitro cytotoxicity

SC4 cells were plated in 96 well plates, at 2500 cells per 100 μ L media. 4 days after plating, following confirmation of partial confluence, lapatinib and nilotinib were individually added in escalating doses with logarithmic scaling, from 10^{-3} to 10^{-7} M. There were at least 6 replicates of each drug dose. Bevacizumab and everolimus were not tested for in vitro cytotoxicity as there are established doses in NF2 models in vivo for both. All media solutions (including controls) contained 1% dimethyl sulfoxide solution (DMSO) solution. The optic density (OD) was measured using an Alamar blue assay (Thermo Fisher Scientific, Waltham, MA) for cell proliferation [31]. The OD results for each dose were compared in logarithmic scale to the OD of the untreated control wells.

In vivo peripheral Schwann cell models

Two in vivo models of tumor cell implantation were utilized: a subcutaneous flank model and a sciatic nerve model, descriptions of implantation techniques for each are described below.

Flank tumor model

Tumor development

Following intraperitoneal anesthesia as described above, the right rostral flank was injected with 1×10^5 cells SC4 cells, trypsinized from cell culture and concentrated in 100 μ L Matrigel (Corning Life Sciences, Tewksbury MA). A long subcutaneous tract was made between the needle penetration and the skin, as well as a purposeful delay in needle withdrawal to prevent tumor cell egress through the needle site. After tumor cell injection the mice were

allowed to recover from anesthesia and were observed daily for toxicity and tumor growth.

Tumor volume/growth assessment

Beginning 3 days after tumor injection the animals were checked daily for palpable tumors. When the tumors were visible and palpable, measurements were recorded in three dimensions—length (L), width (W), and height (H) with manual calipers by a single operator. The formula used to calculate for tumor volume was $(L \times W \times H)/2$. For every experiment, when a significant number of the animals had palpable tumors, allocation to study groups was performed to ensure that animals with no palpable tumor or with tumors larger than two standard deviations from the overall mean were removed from the experiment. After group allocation, treatment was started. Following the onset of experimental treatment, flank tumor measurements occurred on alternate days and volume and growth rate for each tumor was calculated.

Monotherapy: drug treatment

40 nu/nu mice were implanted with SC4 flank tumor as described above. After 5 days, 37 mice had palpable tumors, and these were allocated to groups. Bevacizumab, everolimus, lapatinib and nilotinib were tested in this experiment. Average tumor volumes for all groups were within one standard deviation from each other at baseline. The five groups included: untreated controls ($n=7$); nilotinib, 75 mg/kg, p.o. daily ($n=8$); lapatinib, 100 mg/kg, p.o. 6 days a week ($n=7$); bevacizumab, 5 mg/kg, injected intravenously twice weekly ($n=7$); and everolimus ($n=8$). Multiple dosing and dosing schedules of everolimus have been reported in the literature, ranging from daily and weekly dosages of 0.05 to 15 mg/kg [32–34]. O'Reilly et al. assessed everolimus pharmacokinetics in mice and rats and found that high, intermittent doses may be more efficacious for the treatment of brain tumors [35]. We therefore, delivered everolimus at a 5 mg/kg, p.o. once weekly dose. Flank tumors were measured and analyzed as described above. Mice were observed daily for drug toxicity. When tumor dimensions exceeded 2 cm in any dimension in one mouse, then all the mice in the group were euthanized. The tumors were then removed from the flank, weighed, and fixed in formaldehyde.

Monotherapy: in vivo RT dose response study and toxicity assessment

11 nu/nu mice were injected with SC4 cells in the flank. 5 days after the injection, following tumor volume measurement the mice were allocated to groups and received one

of five possible RT doses: 0 Gy (n=2), 2 Gy (n=2), 5 Gy (n=3), 10 Gy (n=2), and 20 Gy (n=2). To receive RT, animals were anesthetized, placed at a fixed distance from the radiation source, and shielded with a square primary collimator (1 cm in diameter) centered over the tumor implantation site. The radiated animals received external beam single-dose radiation treatment using a Cesium Mark 1 model 68 rodent irradiator (J.L. Shepherd, San Fernando, California). Tumors were measured with manual calipers every second day. Tumor growth, expressed as final tumor volume divided by tumor volume at randomization, was plotted against the dose of radiation. When tumor dimensions exceeded 2 cm in any dimension, all the mice in the group were euthanized. The tumors were then removed, weighed, and fixed in formaldehyde.

Mice were observed daily for focal or systemic radiation toxicity. RT toxicity was assessed for focal factors such as implantation wound breakdown, local necrosis or skin erosion, and for systemic symptoms such as diarrhea, and decreased alertness. This assessment was performed daily by the laboratory and animal facility veterinarian staff. Toxicity assessment was continued for the duration of each experiment.

Treatment: in vivo combination modalities—RT+ drug treatment

SC4 cells were injected into the flank of 45 anesthetized nu/nu mice. 6 days later tumors were measured, tumor volumes were calculated and animals were placed in groups. In this experiment we focused on lapatinib or nilotinib combined with radiation based on their performance as a monotherapy. The dose of radiation was 3 Gy, which was found in the radiation monotherapy experiment to delay tumor growth rate and not to induce toxicity. All tumor sizes were within one standard deviation of the overall mean at baseline. The experiment included the following six groups: untreated control (n=7); RT only, 3 Gy (n=7); nilotinib only, 50 mg/kg, p.o. daily (n=7); lapatinib only, 50 mg/kg, p.o. 6 days a week (n=7); nilotinib, 50 mg/kg, p.o. daily and RT, 3 Gy (n=7); and lapatinib, 50 mg/kg, p.o. 6 days a week and RT, 3 Gy (n=7). Optimal doses of drugs and RT were based on the results from the monotherapy experiments described above. Manual caliper measurements were performed for tumor volume every second day. Mice were assessed daily for drug and radiation toxicity—both systemic and focal.

Sciatic nerve model

Tumor development

45 nu/nu mice were anesthetized with an intraperitoneal (IP) injection of a stock solution containing ketamine

hydrochloride, 75 mg/mL (Ketathesia, Butler Animal Health Supply; Dublin, OH); xylazine 7.5 mg/mL (Lloyd Laboratories; Shenandoah, Iowa), and 14.25% ethyl alcohol in 0.9% NaCl. The animal was placed in a prone position and restrained with the hind legs positioned at 90 degree angles. A horizontal skin incision was made rostral to the tail stem. The gluteal muscles were dissected to isolate the sciatic nerve. SC4 cells trypsinized from cell culture and concentrated at 1×10^5 cells/100 μ l in Matrigel (BD Biosciences, San Jose, CA) were injected in and around the exposed sciatic nerve. The fascia and adjoining muscles were closed with absorbable suture and the skin was closed with stainless steel autoclips. The animals were observed daily for surgical recovery and toxicity.

Tumor volume/growth assessment

Five days after tumor cell injection animals received an IP injection of luciferin, 0.1 mg per mouse (Gold Biotechnology, St. Louis, MO). 8 days after tumor cell injection the animals were imaged using the IVIS Xenogen Imaging System (Xenogen Corporation, Alameda, CA) to confirm presence of tumor. Treatment was started when there was visible tumor in at least 80% of the animals.

Treatment: drug treatment

In vivo combination modalities: RT+ drug treatment 45 nu/nu mice were injected with SC4 tumor in the sciatic nerve. In this experiment we tested the most efficacious chemo-radiation pairs in order to confirm the accuracy of the flank model. Luciferase imaging conducted 8 days after tumor injection showed tumor growth in 37/45 animals. These animals were randomized to the following groups: an untreated control (n=6); RT only, single fraction, 3 Gy (n=5); nilotinib only, 50 mg/kg, was p.o. daily (n=6); lapatinib only, 50 mg/kg, was p.o. 6 days a week (n=6); nilotinib, 50 mg/kg, was p.o. daily, and RT, single fraction, 3 Gy (n=7); lapatinib, 50 mg/kg, was p.o. 6 days a week and RT, single fraction, 3 Gy (n=7). On the ninth day of treatment the mice were imaged again using the IVIS imaging system to document tumor change. Mice were assessed daily for toxicity, including wound breakdown, local necrosis or skin erosion, diarrhea, and decreased alertness. Toxicity assessment was continued for the duration of each experiment. After 15 days of treatment the animals were euthanized and the tumors were resected from the sciatic nerve, weighed and fixed in formaldehyde, paraffin embedded, and stained with hematoxylin and eosin, to confirm PNST morphology. Specimens were reviewed by both a certified neuropathologist (FJR) and a neurosurgeon (IP).

Statistical analysis

Tumor volume at day 15 of treatment was the primary endpoint. A generalized linear model was used for among group comparison for tumor volume difference at a time point. Two sample T-test and a paired T-test were used for between group and within group comparison. The tumor growth rate over time was estimated using a linear regression model. Results with a p value <0.05 were considered statistically significantly different. All statistical tests are two-sided.

Short-term treatment versus extended treatment

To assess the growth of PNST after cessation of therapeutic treatment, 5 days after SC4 cells were injected into the flanks of 23 nu/nu mice, the mice were allocated to treatment groups in the manner described above and randomized to: untreated controls ($n=8$); short term nilotinib (50 mg/kg, p.o. daily for 8 days, $n=7$) and long term nilotinib (50 mg/kg, p.o. daily for 21 days, $n=8$) with RT (3 Gy). Tumor volumes were measured every second day and animals were euthanized when the tumor volume exceeded 2 cm in any dimension. Mice were assessed daily for drug toxicity. After the animals were euthanized, the tumors were removed, weighed, and fixed in formalin.

Pathology and immunohistochemistry

At the conclusion of all experiments, mice were euthanized, and tumors dissected from either the sciatic compartment or the subcutaneous compartment and weighed. All tumors were then fixed in formalin, embedded in paraffin, and sectioned into 10 μm sections. Hematoxylin and eosin (H&E) stains were performed to verify nerve sheath tumor histology. S100 staining was performed on paraffin embedded unstained slides using a commercial antibody (4C4.9, prediluted; Ventana Medical Systems, Tucson, AZ). This stain has been shown to be directed against S100 for confirmation of PNST pathology [36]. All pathology and immunohistochemistry results were reviewed by a blinded neuropathologist (FJR).

Results

Cytotoxicity results

The SC4 cell line was sensitive to external beam radiation treatment, and a consistent dose–response curve was reached (Fig. 1a). The concentration of a single dose of radiation, lethal to 50% of the SC4 cells (LC_{50}), was 6.6 Gy. The SC4 schwannoma cell line also showed sensitivity to

both lapatinib and nilotinib (Fig. 1b, c, respectively) resulting in a 50% inhibition of proliferation (IC_{50}) at 3.1 μM lapatinib and 1.45 μM nilotinib.

In vivo tumor models: flank versus sciatic nerve

The two in vivo models of tumor cell implantation that were utilized, the flank tumor model and the sciatic nerve model, were compared to each other and did not show a statistical difference in tumor growth rate or size within 14 days of implantation ($p=0.9748$). Average tumor weights upon excision were 0.3082 ± 0.061 g (95% CI 0.23–0.38) for those injected in the sciatic nerve and 0.306 ± 0.137 g (95% CI 0.14–0.48) for those injected in the flank.

Radiation monotherapy: flank model

Flank tumor volume measurements following single exposure to an external beam radiation dose of 2 Gy resulted in tumors that grew by over 17-fold. Single exposure to a dose of 5 Gy nearly completely arrested tumor growth. Therefore, a radiation dose of 3 Gy was used for the therapeutic combination studies in order to allow observation of possible additive or synergistic effects with chemoradiation. No toxicity was observed from the focal irradiation at any dose.

Drug monotherapy: flank model

Both nilotinib and lapatinib significantly reduced tumor growth rate when compared to the untreated control group ($p=0.0062$ and $p=0.0025$, respectively) (Fig. 2). Tumor volume on Day 13 was $227 \text{ mm}^3 \pm 125.0 \text{ mm}^3$ for the untreated control, $45.62 \text{ mm}^3 \pm 41.5 \text{ mm}^3$ after lapatinib, and $57.8 \text{ mm}^3 \pm 37.8 \text{ mm}^3$ after nilotinib. The other two compounds tested, bevacizumab and everolimus, showed a trend toward decreasing tumor volume with final tumor volumes of $147.3 \text{ mm}^3 \pm 84.2 \text{ mm}^3$ and $157.8 \text{ mm}^3 \pm 90.3 \text{ mm}^3$, respectively. However, they were not statistically better than the untreated control group ($p=0.14$ for bevacizumab and $p=0.17$ for everolimus), nor were they better at reducing tumor volume than nilotinib ($p=0.018$ vs. bevacizumab, $p=0.017$ vs. everolimus) or lapatinib ($p=0.02$ vs. bevacizumab, $p=0.015$ vs. everolimus). We did not observe any toxicity of the drugs tested in this in vivo model.

In vivo combined radiation and drug efficacy: flank tumor model

There was a statistically significant difference of flank tumor growth rates among the groups that received RT, lapatinib, or nilotinib and with either drug in combination

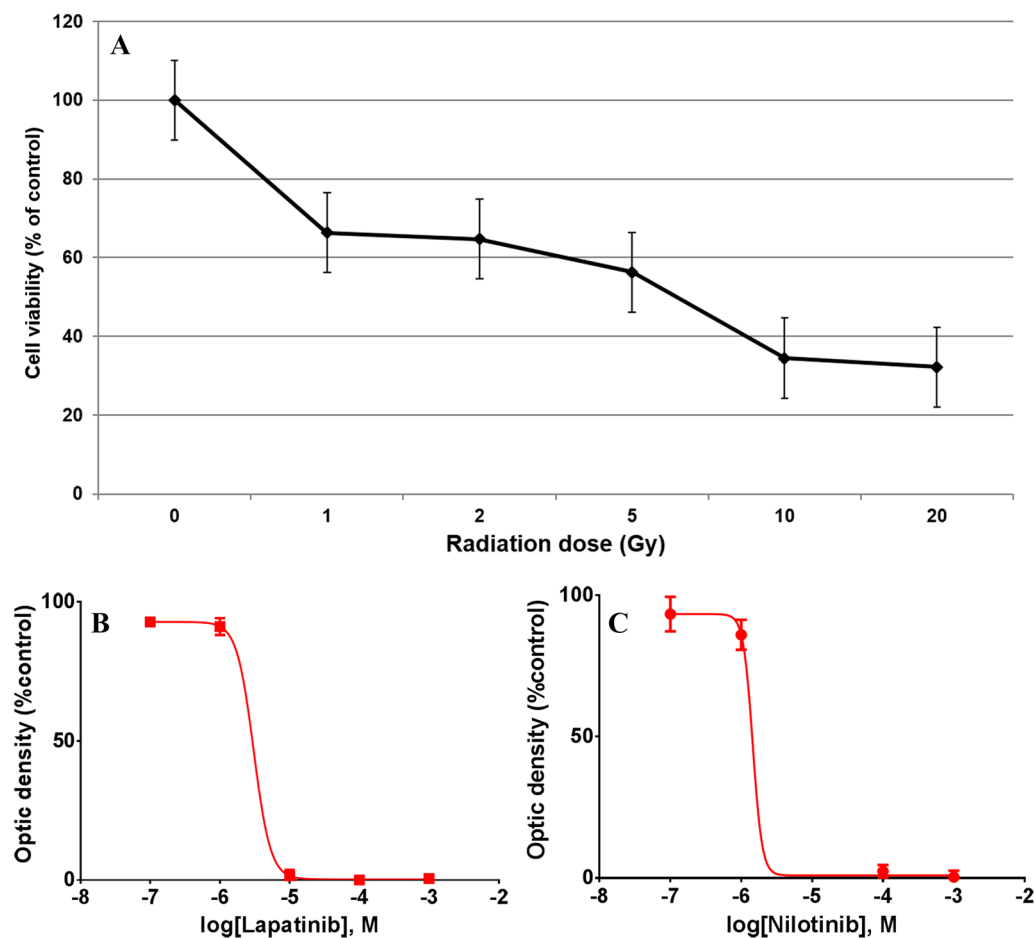


Fig. 1 In vitro cell viability. In vitro SC4 cell dose response curves after treatment with escalating (a) radiation doses, (b) lapatinib, and (c) nilotinib. All data presented as cell viability (% of control) per treatment as assessed by Alamar blue assay

with RT ($p=0.0006$) (Fig. 3). Treatment with nilotinib alone resulted in a significantly slower rate of tumor growth than untreated control, $p<0.05$. A significantly slower growth rate was also seen with both lapatinib plus radiation and nilotinib plus radiation, as compared to the untreated controls ($p<0.05$). Tumor growth rate was also significantly slower in the combination groups as compared to the groups receiving either RT or drug alone (Fig. 3). With radiation alone, lapatinib alone, or nilotinib alone, tumors were 54% smaller at day 15 compared to the control group. The average reduction in tumor growth rate was 92% in the RT+ lapatinib and 92% in the RT+ nilotinib groups as compared to the control. We observed no toxicity from either of the drugs or the radiation in this experiment.

Short-term treatment versus extended treatment

In a sub-experiment, animals with flank tumors were treated with radiation and nilotinib, with nilotinib treatment given for either 8 days ($n=8$) or until the end of the

experiment at 21 days ($n=8$). Throughout the experiment, the short term (8 day) treatment group and the long term (21 day) treatment group remained statistically similar, $p=0.82$ for rate of tumor growth over 21 days, and $p=0.89$ for final tumor size on Day 21 at the end of the experiment. Similarly, average tumor volumes on Day 19 were 20.9 mm^3 for the short term nilotinib+ radiation group and 23.3 mm^3 for mice in the long term nilotinib+ radiation group (Fig. 4). In comparison, the average tumor volume on day 13 for the untreated control group was 279 mm^3 . We observed no toxicity of any of the drugs or the radiation in this experiment.

Sciatic nerve model

Combined radiation and drug efficacy In order to confirm the results in the flank model, we tested the best performers (lapatinib and nilotinib) in the sciatic nerve model. Continuous measurement was not possible in the deep compartment of the sciatic nerve tumor model. Therefore a single meas-

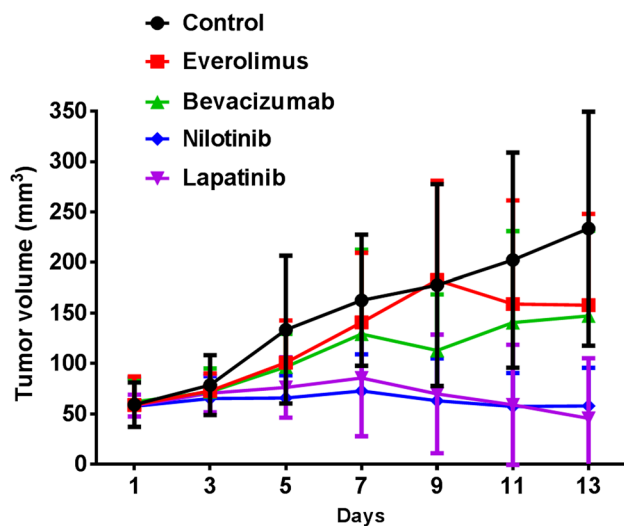


Fig. 2 In vivo monotherapy in SC4 implanted flank tumors. Average tumor volume over time following exposure to different treatments: untreated control (*black circle* $n=7$), everolimus (*red square* $n=8$), bevacizumab (*green triangle* $n=7$), nilotinib (*blue diamond* $n=8$), and lapatinib (*purple inverted triangle* $n=7$)

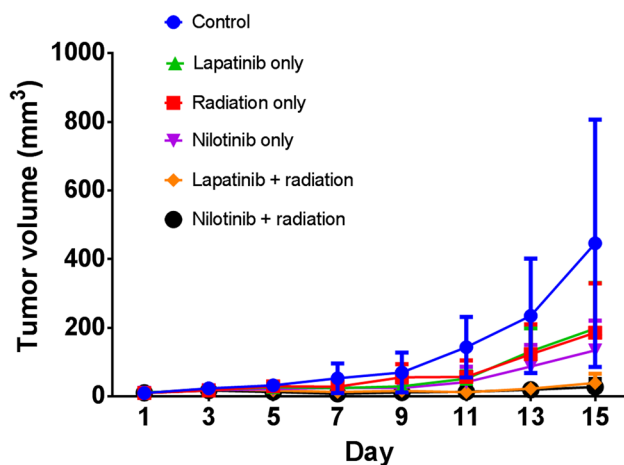


Fig. 3 Chemoradiation in the SC4 flank tumor model. Averages flank tumor volume over time following exposure to combination therapy: untreated control (*blue circle* $n=7$), lapatinib only (*green triangle* $n=7$), radiation only, 3 Gy (*red square* $n=7$), nilotinib only (*purple inverted triangle* $n=7$), lapatinib + radiation, 3 Gy (*orange diamond* $n=7$) and nilotinib + radiation, 3 Gy (*black circle* $n=7$)

urement of the excised tumor weight was used to calculate final tumor volume after radiation and drug treatment. Treatment of the sciatic nerve tumor with nilotinib alone, lapatinib alone, or radiation alone all led to a significant reduction in tumor growth rate versus control ($p<0.05$, Fig. 5). The average tumor weights upon tumor excision on Day 15 were: control 2.44 ± 0.98 g; radiation only 1.11 ± 0.44 g; lapatinib only 1.07 ± 0.40 g; nilotinib only 1.11 ± 0.44 g;

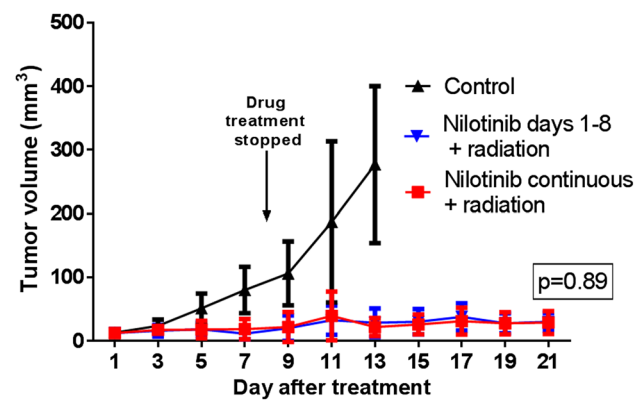


Fig. 4 Long term versus short term nilotinib treatment in the SC4 flank model. Tumor volume growth over time following flank tumor implantation and exposure to different treatments: untreated control (*black triangle*), short term (8 days) nilotinib treatment + radiation (*blue inverted triangle*) and long term nilotinib (21 days) + radiation (*red square*)

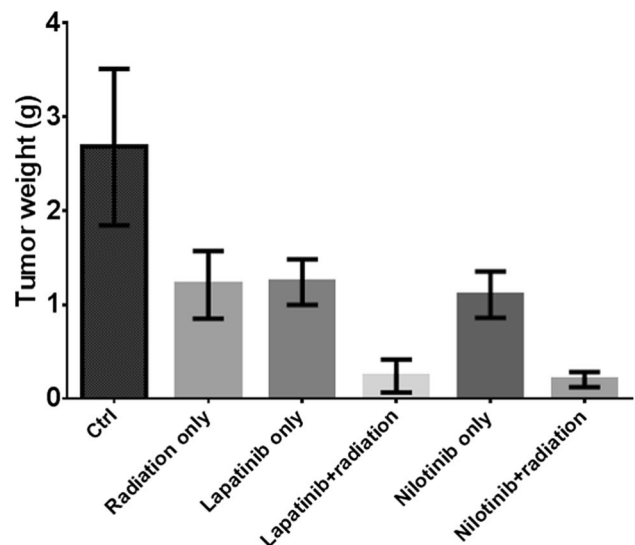


Fig. 5 Chemoradiation in the SC4 sciatic nerve model. Animals implanted in the sciatic nerve with SC4 cells received one of the following treatments: untreated control, radiation only, lapatinib only, lapatinib + radiation, nilotinib only, and nilotinib + radiation. On Day 15, tumors were excised and weighed (g)

lapatinib + radiation 0.56 ± 0.46 g; nilotinib + radiation 0.20 ± 0.07 g.

Luciferase-based immunofluorescence of the sciatic nerve tumors was observed for each treatment group (data not shown). There were no differentiating features of aggressive pathology between the histological sections of untreated control tumors and tumors from animals treated with any modality, as determined by a neuropathologist (FJR). We observed no toxicity of any of the drugs or the radiation in this experiment.

Pathology and immunohistochemistry

Since the SC4 tumor had not previously been characterized *in vivo*, pathological and immunohistochemical evaluations were conducted. Histological sections demonstrated well circumscribed spindle cell neoplasms with hypercellularity and brisk mitotic activity. Necrosis with a pseudopalisading quality was present in two of the ten specimens. All tumors expressed S100 protein consistent with a Schwann cell lineage. Extent of expression varied from strong (+++) ($n=4$) to partial (++) ($n=4$) or rare cells (+) ($n=2$). These findings are consistent with a cellular spindle cell neoplasm with an immunophenotype consistent with Schwann cell lineage. There were no differences in the histological phenotype between the irradiated tumors and those that had not been irradiated.

Discussion

Therapeutic options for the treatment of peripheral schwannomas are limited [37]. Patients with either NF2 or schwannomatosis have significant morbidity due to peripheral nerve sheath tumors. NF2 associated schwannomas and schwannomatosis are genetically unique and result in varying anatomic distribution of lesions, clinical presentation, medical management, and patient outcomes [38]. Schwannomatosis rarely results in vestibular schwannomas or meningiomas [38]. The current treatment schemes consist of management of tumor associated symptoms, resection, or rarely, RT for tumors not amenable to resection [39]. RT has also been used for the treatment of VS, however, with overall less efficacy and concerns for a higher rate of long-term toxicity in the setting of NF2 [40]. Several drug therapies have been considered potentially beneficial in growth restriction of schwannomas, based on their potential to inhibit tumorigenic targets. These trials have focused on VS and not peripheral schwannomas.

Recently, Giovannini et al. [15] demonstrated a decrease in the size of paraspinal schwannomas when tumors were treated with rapamycin, an MTORc1 inhibitor. Our efficacy results with a rapalog, everolimus, and SC-4 cells were not as impressive. The mechanism of tumor implantation, method of tumor measurement, the use of a different agent, dosing, and scheduling protocols (weekly instead of daily) all may account for this difference in efficacy.

In our studies we employed two *in vivo* models of peripheral schwannoma: one located in the murine flank and one injected into the murine sciatic nerve. Both models have benefits as well as limitations. The main advantage of the *in vivo* flank model is that the tumor is readily accessible for continuous measurement. The availability for quantification enables allocation of animals to equal

tumor-volume treatment groups and repeated tumor volume measurements throughout the experiment in real-time, allowing quantification of tumor volumes for therapeutic dose response studies. However, a limitation of this model is that it is not as physiologically relevant as the sciatic nerve model. The sciatic nerve model more closely models PNST growth, the impact of the microenvironment, and allows for functional assessments such as neurologic morbidity related to tumor growth, similar to that observed clinically. The disadvantage of sciatic compartment tumor localization is that it is not amenable to continuous measurements and is more technically challenging which can impact reproducibility.

Since both models have benefits and limitations, we compared the two models directly, testing the combined treatment of drugs and radiation (Figs. 3 and 5). We showed that the growth of the tumors in the flank closely resembles tumor growth on the peripheral nerve sheath, and that the results in both models, using various treatment conditions, are similar.

The SC4 cell line is a genetically modified mouse model of NF2 related Schwann cell lineage line with an $Nf2^{-/-}$ genotype, derived from a mouse adult cell line that has been studied extensively as a model for NF2 schwannomas [15, 41–45]. The tumors produced *in vivo* from SC4 cells had several features consistent with classical benign schwannoma, however, they also had some histological features suggestive of a more aggressive nature, including high mitotic activity and necrosis in some of the specimens. Hence, we conclude that this cell line is a reproducible model for peripheral schwannomas with NF2 deletion with feasible utility in the lab but with some more aggressive growth features characteristic of mouse PNST [46]. The relatively brief doubling time of these cells was also useful for straightforward experimental design and reproducibility. We found no difference in the histological phenotype which may have been suggestive of radiation-induced malignant transformation in lesions followed for 100 days after treatment.

Interestingly, although bevacizumab and everolimus have the greatest amount of evidence for activity in VS in clinical trials, their efficacy was equivalent to control in our flank tumor model. Some technical limitations may have affected the efficacy of these drugs. The limited efficacy of bevacizumab may be attributed to specificity to human VEGF, and may thus have resulted in reduced efficacy in this nude mouse model. The efficacy of utilizing an anti-angiogenic agent is unclear. Furthermore, although the dose and dosing schedule of both bevacizumab and everolimus are based on previous data, these dosages are not as established for rodents. Multiple doses and dosing schedules have been described in the literature. In contrast, both nilotinib and lapatinib showed

activity as monotherapy and then enhanced activity when given concordantly with RT. Lapatinib has also been tested clinically for NF2 associated VS, but the activity against extracranial PNST was not assessed.

An important finding of this study was that there was no acute radiation toxicity observed from RT at doses up to 20 Gy. As described, the form of radiation given was focal and single dose, and the untreated areas in the mouse body were appropriately shielded from radiation. This factor may explain the lack of systemic radiation toxicity, however, we observed no focal toxicity either. There was no skin injury, atrophy of the area, or focal necrosis. Additionally the area of previous surgery seemed unaffected by radiation in the doses tested. We also noted no toxicity attributable to the drugs given in the doses described. Our results suggest that there may be better efficacy for NF2 associated PNST than may have been expected based on the existing data regarding activity in NF2 associated VS. However, the relatively short experimental window of our preclinical models cannot fully predict the range of toxicity that may be experienced when applying RT for NF2 associated PNST, including late risk of malignant conversion. Nevertheless, there were no such cases during an observation window of up to 100 days in this study. The combinations of lapatinib and RT and nilotinib and RT were impressive in our two independent in vivo models. In future studies, due to this combinatorial increased effect, it might be possible to decrease the dosage of chemotherapy when combined with RT to achieve a similarly impressive effect. To achieve similar control rates for NF2 vestibular schwannomas compared to sporadic vestibular schwannomas, increased dosage of RT is necessary which leads to increased complications [47, 48]. Concomitant effective targeted therapies may result in lower dosages of RT delivered, thereby decreasing their associated toxicities. Future studies could be aimed at verifying this possible benefit.

Also, nilotinib had sustained activity even after cessation of treatment. If this effect is replicated in human subjects, then treatment may potentially be given short term or in “pulse doses” to improve tolerance while maintaining efficacy. In this model for PNST in NF2, nilotinib and lapatinib, both in combination with radiation and as monotherapy were significantly better at reducing tumor growth than untreated controls. Monotherapy with lapatinib or nilotinib was also better than bevacizumab or everolimus for these PNST. These results suggest that concurrent low dose RT and targeted therapy with agents such as nilotinib and lapatinib should be considered as possible candidates for treatment options in addressing progressive PNST in patients with NF2.

Acknowledgements We thank Mr. and Mrs. Peter Jennison for their kind and generous support. We would also like to thank Eden Paldor for her technical assistance.

References

1. Lloyd SK, Evans DG (2013) Neurofibromatosis type 2 (NF2): diagnosis and management. *Handb Clin Neurol* 115:957–967
2. Evans DG (2009) Neurofibromatosis type 2 (NF2): a clinical and molecular review. *Orphanet J Rare Dis* 4:16
3. Stamenkovic I, Yu Q (2010) Merlin, a “magic” linker between extracellular cues and intracellular signaling pathways that regulate cell motility, proliferation, and survival. *Current Protein Pept Sci* 11(6):471–484
4. Lee JY, Kim H, Ryu CH et al (2004) Merlin, a tumor suppressor, interacts with transactivation-responsive RNA-binding protein and inhibits its oncogenic activity. *J Biol Chem* 279(29):30265–30273
5. Hamaratoglu F, Willecke M, Kango-Singh M et al (2006) The tumour-suppressor genes NF2/Merlin and Expanded act through Hippo signalling to regulate cell proliferation and apoptosis. *Nat Cell Biol* 8(1):27–36
6. Wong HK, Shimizu A, Kirkpatrick ND et al (2012) Merlin/NF2 regulates angiogenesis in schwannomas through a Rac1/semaforin 3F-dependent mechanism. *Neoplasia* 14(2):84–94
7. Plotkin SR, Merker VL, Muzikansky A, Barker FG 2nd, Slattery W 3rd (2014) Natural history of vestibular schwannoma growth and hearing decline in newly diagnosed neurofibromatosis type 2 patients. *Otol Neurotol* 35(1):e50–e56
8. Paldor I, Chen AS, Kaye AH (2016) Growth rate of vestibular schwannoma. *J Clin Neurosci* 32:1–8. doi:10.1016/j.jocn.2016.05.003
9. Elsharkawy M, Xu Z, Schlesinger D, Sheehan JP (2012) Gamma Knife surgery for nonvestibular schwannomas: radiological and clinical outcomes. *J Neurosurg* 116(1):66–72
10. Blakeley JO, Ye X, Duda DG et al (2016) Efficacy and biomarker study of bevacizumab for hearing loss resulting from neurofibromatosis type 2-associated vestibular schwannomas. *J Clin Oncol* 34(14):1669–1675
11. Voss MH, Molina AM, Motzer RJ (2011) mTOR inhibitors in advanced renal cell carcinoma. *Hematol/Oncol Clin North Am* 25(4):835–852
12. Fonseca PJ, Uriol E, Galvan JA et al (2013) Prolonged clinical benefit of everolimus therapy in the management of high-grade pancreatic neuroendocrine carcinoma. *Case Rep Oncol* 6(2):441–449
13. Villarreal-Garza C, Cortes J, Andre F, Verma S (2012) mTOR inhibitors in the management of hormone receptor-positive breast cancer: the latest evidence and future directions. *Ann Oncol* 23(10):2526–2535
14. Johansson G, Mahller YY, Collins MH et al (2008) Effective in vivo targeting of the mammalian target of rapamycin pathway in malignant peripheral nerve sheath tumors. *Mol Cancer Ther* 7(5):1237–1245
15. Giovannini M, Bonne NX, Vitte J et al (2014) mTORC1 inhibition delays growth of neurofibromatosis type 2 schwannoma. *Neuro Oncol* 16(4):493–504
16. Karajannis MA, Legault G, Hagiwara M et al (2014) Phase II study of everolimus in children and adults with neurofibromatosis type 2 and progressive vestibular schwannomas. *Neuro Oncol* 16(2):292–297
17. Goutagny S, Raymond E, Esposito-Farese M et al (2015) Phase II study of mTORC1 inhibition by everolimus in neurofibromatosis

- type 2 patients with growing vestibular schwannomas. *J Neurooncol* 122(2):313–320
18. Guarneri V, Generali DG, Frassoldati A et al (2014) Double-blind, placebo-controlled, multicenter, randomized, phase IIb neoadjuvant study of letrozole-lapatinib in postmenopausal hormone receptor-positive, human epidermal growth factor receptor 2-negative, operable breast cancer. *J Clin Oncol* 32(10):1050–1057
 19. Ammoun S, Cunliffe CH, Allen JC et al (2010) ErbB/HER receptor activation and preclinical efficacy of lapatinib in vestibular schwannoma. *Neuro Oncol* 12(8):834–843
 20. Ahmad ZK, Brown CM, Cueva RA, Ryan AF, Doherty JK (2011) ErbB expression, activation, and inhibition with lapatinib and tyrphostin (AG825) in human vestibular schwannomas. *Otol Neurotol* 32(5):841–847
 21. Karajannis MA, Legault G, Hagiwara M et al (2012) Phase II trial of lapatinib in adult and pediatric patients with neurofibromatosis type 2 and progressive vestibular schwannomas. *Neuro Oncol* 14(9):1163–1170
 22. Jabbour E, Kantarjian H (2014) Chronic myeloid leukemia: 2014 update on diagnosis, monitoring, and management. *Am J Hematol* 89(5):547–556
 23. Cauchi C, Somaiah N, Engstrom PF et al (2012) Evaluation of nilotinib in advanced GIST previously treated with imatinib and sunitinib. *Cancer Chemother Pharmacol* 69(4):977–982
 24. Ammoun S, Schmid MC, Triner J, Manley P, Hanemann CO (2011) Nilotinib alone or in combination with selumetinib is a drug candidate for neurofibromatosis type 2. *Neuro Oncol* 13(7):759–766
 25. Blakeley JO, Evans DG, Adler J et al (2012) Consensus recommendations for current treatments and accelerating clinical trials for patients with neurofibromatosis type 2. *Am J Med Genet Part A* 158A(1):24–41
 26. Lim DJ, Rubenstein AE, Evans DG et al (2000) Advances in neurofibromatosis 2 (NF2): a workshop report. *J Neurogenet* 14(2):63–106
 27. Seferis C, Torrens M, Paraskevopoulou C, Psychidis G (2014) Malignant transformation in vestibular schwannoma: report of a single case, literature search, and debate. *J Neurosurg* 121:160–166
 28. Vuletic I, Zhou K, Li H et al (2017) Validation of bevacizumab therapy effect on colon cancer subtypes by using whole body imaging in mice. *Mol Imaging Biol*. doi:[10.1007/s11307-017-1048-z](https://doi.org/10.1007/s11307-017-1048-z)
 29. Ishikura N, Yanagisawa M, Noguchi-Sasaki M et al (2017) Importance of bevacizumab maintenance following combination chemotherapy in human non-small cell lung cancer xenograft models. *Anticancer Res* 37(2):623–629
 30. Tai CJ, Wang H, Wang CK et al (2017) Bevacizumab and cetuximab with conventional chemotherapy reduced pancreatic tumor weight in mouse pancreatic cancer xenografts. *Clin Exp Med* 17(2):141–150
 31. Nakayama GR, Caton MC, Nova MP, Parandoosh Z (1997) Assessment of the Alamar Blue assay for cellular growth and viability in vitro. *J Immunol Methods* 204(2):205–208
 32. Pawaskar DK, Straubinger RM, Fetterly GJ et al (2013) Physiologically based pharmacokinetic models for everolimus and sorafenib in mice. *Cancer Chemother Pharmacol* 71(5):1219–1229
 33. Pawaskar DK, Straubinger RM, Fetterly GJ et al (2013) Synergistic interactions between sorafenib and everolimus in pancreatic cancer xenografts in mice. *Cancer Chemother Pharmacol* 71(5):1231–1240
 34. Cejka D, Kuntner C, Preusser M et al (2009) FDG uptake is a surrogate marker for defining the optimal biological dose of the mTOR inhibitor everolimus in vivo. *Br J Cancer* 100(11):1739–1745
 35. O'Reilly T, McSheehy PM, Kawai R et al (2010) Comparative pharmacokinetics of RAD001 (everolimus) in normal and tumor-bearing rodents. *Cancer Chemother Pharmacol* 65(4):625–639
 36. Rodriguez FJ, Folpe AL, Giannini C, Perry A (2012) Pathology of peripheral nerve sheath tumors: diagnostic overview and update on selected diagnostic problems. *Acta Neuropathol* 123(3):295–319
 37. Rowe JG, Radatz MW, Walton L, Hampshire A, Seaman S, Kemeny AA (2003) Gamma knife stereotactic radiosurgery for unilateral acoustic neuromas. *J Neurol Neurosurg Psychiatry* 74(11):1536–1542
 38. Koontz NA, Wiens AL, Agarwal A et al (2013) Schwannomatosis: the overlooked neurofibromatosis? *Am J Roentgenol* 200(6):W646–53
 39. Rowe J, Radatz M, Kemeny A (2008) Radiosurgery for type II neurofibromatosis. *Prog Neurol Surg* 21:176–182
 40. Gao X, Zhao Y, Stemmer-Rachamimov AO, Liu H, Huang P, Chin S, Selig MK, Plotkin SR, Jain RK, Xu L (2015) Anti-VEGF treatment improves neurological function and augments radiation response in NF2 schwannoma model. *Proc Natl Acad Sci USA* 112(47):14676–81. doi:[10.1073/pnas.1512570112](https://doi.org/10.1073/pnas.1512570112)
 41. Messerli SM, Tang Y, Giovannini M, Bronson R, Weissleder R, Breakefield XO (2002) Detection of spontaneous schwannomas by MRI in a transgenic murine model of neurofibromatosis type 2. *Neoplasia* 4(6):501–509
 42. Jessen WJ, Miller SJ, Jousma E et al (2013) MEK inhibition exhibits efficacy in human and mouse neurofibromatosis tumors. *J Clin Invest* 123(1):340–347
 43. Giovannini M, Robanus-Maandag E, van der Valk M et al (2000) Conditional biallelic Nf2 mutation in the mouse promotes manifestations of human neurofibromatosis type 2. *Genes Dev* 14(13):1617–1630
 44. Messerli SM, Prabhakar S, Tang Y et al (2006) Treatment of schwannomas with an oncolytic recombinant herpes simplex virus in murine models of neurofibromatosis type 2. *Hum Gene Ther* 17(1):20–30
 45. Tanaka K, Eskin A, Chareyre F et al (2013) Therapeutic potential of HSP90 inhibition for neurofibromatosis type 2. *Clin Cancer Res* 19(14):3856–3870
 46. Stemmer-Rachamimov AO, Louis DN, Nielsen GP, Antonescu CR, Borowsky AD, Bronson RT, Burns DK, Cervera P, McLaughlin ME, Reifengerger G, Schmale MC, MacCollin M, Chao RC, Cichowski K, Kalamirides M, Messerli SM, McClatchey AI, Niwa-Kawakita M, Ratner N, Reilly KM, Zhu Y, Giovannini M (2004) Comparative pathology of nerve sheath tumors in mouse models and humans. *Cancer Res* 64(10):3718–3724
 47. Wagner J, Welzel T, Habermehl D, Debus J, Combs SE (2014) Radiotherapy in patients with vestibular schwannoma and neurofibromatosis type 2: clinical results and review of the literature. *Tumori* 100(2):189–194. doi:[10.1700/1491.16411](https://doi.org/10.1700/1491.16411)
 48. Phi JH, Kim DG, Chung HT, Lee J, Paek SH, Jung HW (2009) Radiosurgical treatment of vestibular schwannomas in patients with neurofibromatosis type 2: tumor control and hearing preservation. *Cancer* 115(2):390–398. doi:[10.1002/cncr.24036](https://doi.org/10.1002/cncr.24036)